Landslides (2014) 11:639–653
DOI 10.1007/s10346-013-0415-3
Received: 10 August 2012
Accepted: 16 May 2013
Published online: 28 July 2013

Dario Costanzo · José Chacón · Christian Conoscenti · Clemente Irigaray · Edoardo Rotigliano

Forward logistic regression for earth-flow landslide susceptibility assessment in the Platani river basin (southern Sicily, Italy)

Abstract Forward logistic regression has allowed us to derive an earth-flow susceptibility model for the Tumarrano river basin, which was defined by modeling the statistical relationships between an archive of 760 events and a set of 20 predictors. For each landslide in the inventory, a landslide identification point (LIP) was automatically produced as corresponding to the highest point along the boundary of the landslide polygons, and unstable conditions were assigned to cells at a distance up to 8m. An equal number of stable cells (out of landslides) was then randomly extracted and appended to the LIPs to prepare the dataset for logistic regression. A model building strategy was applied to enlarge the area included in training the model and to verify the sensitivity of the regressed models with respect to the locations of the selected stable cells. A suite of 16 models was prepared by randomly extracting different unoverlapping stable cell subsets that have been appended to the unstable ones. Models were finally submitted to forward logistic regression and validated. The results showed satisfying and stable error rates (0.236 on average, with a standard deviation of 0.007) and areas under the receiver operating characteristic (ROC) curve (AUCs) (0.839 for training and 0.817 for test datasets) as well as factor selections (ranks and coefficients). As regards the predictors, steepness and large-profile and local-plan topographic curvatures were systematically selected. Clayey outcropping lithology, midslope drainage, local and midslope ridges, and canyon landforms were also very frequently (from eight to 15 times) included in the models by the forward selection procedures. The model-building strategy allowed us to produce a performing earth-flow susceptibility model, whose model fitting, prediction skill, and robustness were estimated on the basis of validation procedures, demonstrating the independence of the regressed model on the specific selection of the stable cells.

Keywords Landslide susceptibility assessment · Forward logistic regression · Diagnostic area · Model validation · Platani river (Sicily Italy)

Introduction

Landslide susceptibility assessment is undoubtedly one of the most debated subjects in recent decades. Many papers are published annually by international journals, which highlight the great interest in the matter for scientific, land management, and civil protection aims (e.g., Aleotti and Chowdhury 1999; Brenning 2005; Chacón and Corominas 2003; Chacón et al. 2006; Guzzetti et al. 1999; Guzzetti et al. 2005). Among the methods that can be followed in assessing the landslide susceptibility, those based on stochastic approaches are gaining increasing importance and number of applications, particularly for basin-scale studies. Stochastic models are based on the definition of statistical relationships which quantitatively and objectively link the spatial distribution of past landslide events to that of a set of geoenvironmental variables. Under the assumption that new landslides will be conditioned by the same factors that caused those in the past, the statistical relationships that links factors to past landslides allow us to produce a prediction image, which spatially depicts the probability for future phenomena: a susceptibility map. This can be, finally, submitted to validation procedures in order to estimate model fitting and adequacy as well as, if a test event inventory (i.e., landslides not used in training the model) is available, prediction skill and robustness. Table 1 gives a summary of the most used statistical techniques together with several associated references for previous applications.

Among the statistical techniques and also in comparative studies (Akgün 2012; Felicísimo et al. 2012; Guzzetti et al. 2005; Mathew et al. 2009; Rossi et al. 2010; Vorpahl et al. 2012), logistic regression (Hosmer and Lemeshow 2000) has proved to be one of the most suitable and performing methods for assessment of landslide susceptibility on basin scale. The wide use of this multivariate technique for landslide susceptibility modeling is mainly due to its capacity to work on any type of independent variable (either ratio, interval, and ordinal or nominal scale), regardless of the deviance of the considered predictors and residuals from a normal distribution. This allows the analyst to manage the model with a more direct and geomorphologically sound approach, without needing to define normally distributed transformed variables. All the discrete independent variables are binarized and transformed into dichotomous or polychotomous variables. The dependent variable is defined as a binary variable in terms of the stable/unstable status of the mapping unit we want to classify.

One of the main problems concerned with using logistic regression is the requirement of balanced dataset, in which the number of stable and unstable cases would be the same. This is obviously rarely verified in real nature (the cumulative extension of the recognized landslides is typically a small fraction of the whole investigated areas), so that typically, together with all the unstable cells, only an equal number of stable cells is randomly singled out from the investigated area; the logistic regression is then run on this very limited subset, often neglecting the larger whole remaining area and assuming the regression equation as representative of it as well.

A test was carried out in a basin of central Sicily to adopt an approach for estimating possible lack in robustness of the susceptibility model due to the limited spatial extension of the actual processed area. The procedure is based on the preparation of a suite of balanced datasets, each including the same unstable cells but different randomly selected stable ones. The forward logistic regression technique is then applied to derive different models, whose performances and structure (type, number, and ranking of predictors) are compared to estimate the robustness of the whole procedure and the results.

Table 1 Resume of the most -adopted statistical techniques for stochastic landslide susceptibility assessment, with some of the previous application cases

Statistical technique	Examples of previous studies
Conditional analysis (CA)	Clerici et al. (2010, Conoscenti et al. (2008, Costanzo et al. (2012a, 2012b), Irigaray et al. (2007), Jiménez-Peralvárez et al. (2009), Rotigliano et al. (2011, 2012), Vergari et al. (2011)
Discriminant analysis (DA)	Baeza and Corominas (2001), Carrara (1983), Carrara et al. (2008), Guzzetti et al. (2006), Rossi et al. (2010.)
Binary logistic regression (BLR)	Atkinson and Massari (1998), Ayalew and Yamagishi (2005), Bai et al. (2010), Can et al. (2005), Carrara et al. (2008), Chauan et al. (2010), Conforti et al. (2012), Dai and Lee (2002), Davis and Ohlmacher (2002), Erener and Düzgün (2010), Mathew et al. (2009), Nandi and Shakoor (2009), Nefeslioglu et al. (2008), Ohlmacher and Davis (2003), Van den Eckhaut et al. (2006, 2009, 2011)
Classification and regression trees (CART)	Felicísimo et al. (2012), Vorpahl et al. (2012)
Artificial neuronal networks (ANN)	Aleotti and Chowdhury (1999), Ermini et al. (2005), Lee et al. (2004), Pradhan and Lee (2010)

Study area

Regional setting

The Tumarrano river basin extends in central-southern Sicily for approximately 80 km² (Fig. 1), having a geological setting which is marked by tectonic contacts between brittle (limestones and quartz arenites) and ductile (clays and silty clays) lithologic complexes, in the northwestern sector; elsewhere, where clays and marls outcrop, smoothed long slopes characterize the landscape. The clayey lithology can be referred to the following lithostratigraphic terms: Numidian Flysch (Upper Oligocene–Lower Miocene), Terravecchia Fm. (Tortonian), and the Castellana Fm. (Serravallian).

The climate of the area is of mild Mediterranean (Csa) type, with mean annual rainfall of 577 mm, which are concentrated in a wet period, between October and April. The soil use in the area is mainly (80 %) characterized by arable lands (corn) and, subordinately, in the extreme northwestern sector, by a dense forest coverage. A very small southern sector is dedicated to pasture.

Landslides

The landslide inventory was prepared (Costanzo et al. 2012a) by a remote Google Earth™-aided recognition survey, exploiting high-resolution images of the area (catalog ID: 1010010008265000, date: Jun. 11, 2008, sensor: QB02, band info: Pan_MS1; catalog ID: 10100100071CDC00, date: Aug. 28, 2007, sensor: QB02, band info: Pan_MS1). Field surveys were also carried out to perform a field check on randomly selected sectors of the studied area. The landslide archive consists of 760 earth flows, mainly involving the clayey and sandy clayey terrains which largely outcrop in the area (Fig. 2).

Earth flow is a very diffused landslide type in Sicily, as large areas are characterized by the outcropping over long, steep slopes of clayey terrains, which can be easily saturated depending on their high sand and/or silt content (>30 %). This condition is responsible for the wide activation of earth flows in the autumn and winter seasons. Landslides in the area have typically shallow failure zones (a few meters maximum, but only 1 m, on average), with a very variable extension: more than 300 cases having an area less than 5,000 m², about 200 in the range 5,000–13,000 m², and 125 in the range 13,000–26,000 m². Earth-flow activation is mainly controlled by soil saturation which results in a lowering of cohesion (for the clayey fraction) and in an increase of neutral pressure inside the saturated voids. The phenomena involve earth or debris type materials taking the form of both open slope and long runout phenomena (Fig. 3).

As regards the status of activity and time recurrence, the slopes affected by landslides have typically seasonal reactivation cycles, characterized, on average, by a maximum of 1- to 2-year dormant stages (Figs. 3 and 4). Therefore, almost all the landslides are to be considered in an active or dormant status; some new activation is subordinately recognized.

Few other types of movement were recognized, which are mainly classifiable as slides or falls. These landslides are not considered in the following section, as this study focuses on flow landslides; besides, the susceptibility assessment of the other types of movement would have required the selection of a different set of controlling factors.

Materials and methods

Model building strategy

Logistic regression aims at modeling a linear relationship between the logit (or log odds) of the outcome and a set of p independent variables or covariates (Hosmer and Lemeshow 2000):

$$g(x) = In\left[\frac{\pi(x)}{1-\pi(x)}\right] = \alpha + \beta_1 x_1 + \beta_2 x_2 + \cdots + \beta_p x_p,$$

where $\pi(x)$ is the conditional mean of the outcome (i.e. the event occurs or unstable slope conditions are found) given the condition x, α is the constant term, the x's are the input predictor variables and the β's are their coefficients. The fitting of the logistic regression model, which is performed by adopting *maximum likelihood estimators*, allows us to estimate the coefficients β_p. In this way, it is possible to predict the outcome from the input predictors and their coefficients.

As the fitting of the model is based on maximizing the value of the likelihood, comparing the likelihood itself allows us to estimate the goodness of different regression models. In particular, by multiplying by −2 the log-likelihood ratio, the *negative log-likelihood* (−2LL) statistic is obtained, which has an approximate *chi square* (x^2) distribution, so that the significance of a difference between the fitting of different models can be estimated in terms of probability of occurrence by chance. The −2LL statistic can be

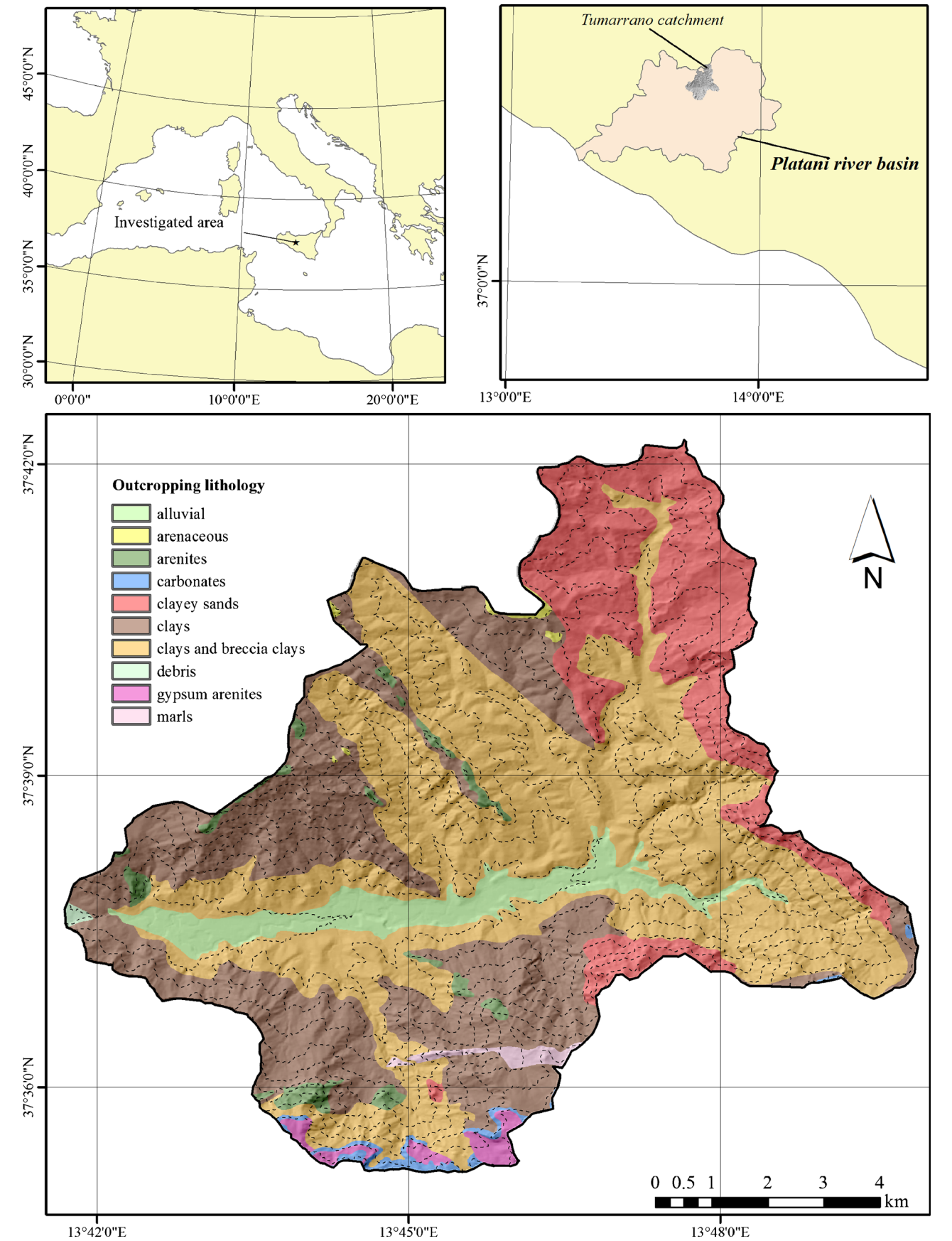

Fig. 1 Location of the Tumarrano river basin (*top*) and lithological map (*bottom*)

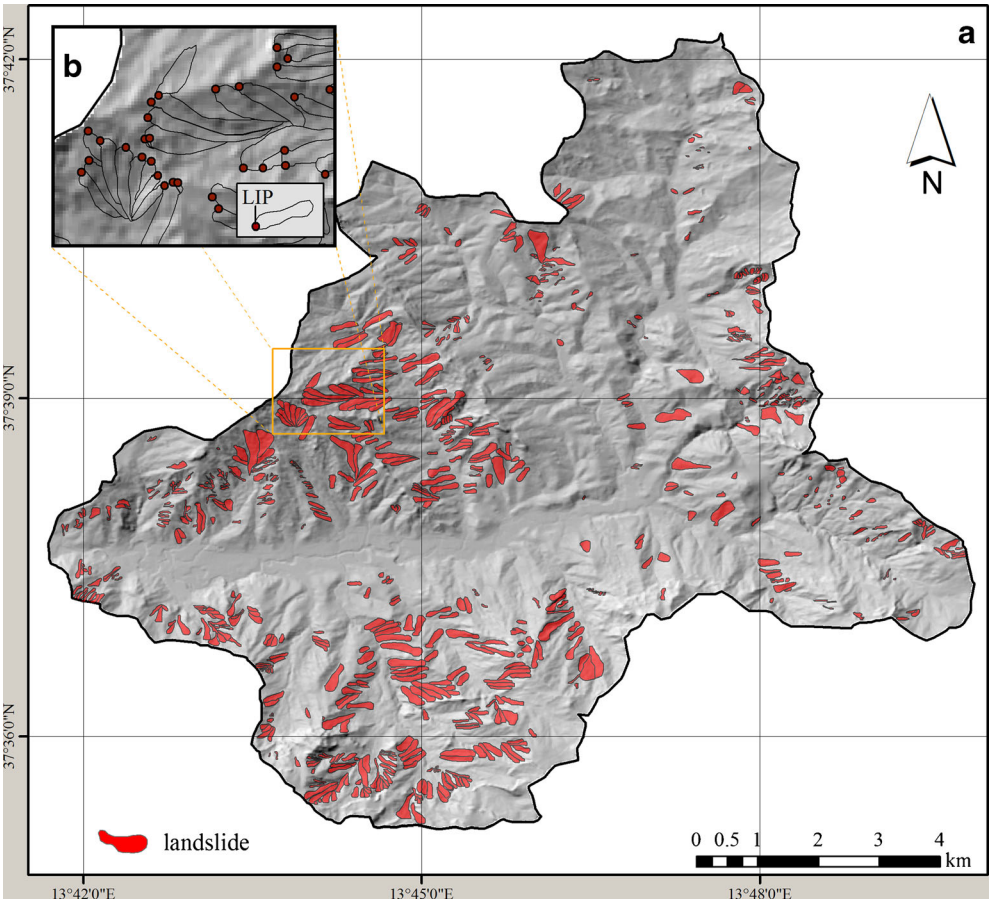

Fig. 2 Earth-flow landslide map (**a**); zoomed detail of landslide identification point (LIP) positioning (**b**)

exploited to compare the fitting of the model having only the constant term (all the β_p are set to 0) with the fitting of the model that includes all the considered predictors with their estimated non-null coefficients so as to verify if the increase in likelihood is significant; in this case, at least one of the *p* coefficients is to be expected as different from zero (Hosmer and Lemeshow 2000).

By exponentiating the β's, odds ratios (OR) for the independent variables are derived: these are measures of association between the independent variables and the outcome of the dependent, and directly express how much more likely (or unlikely) it is for the outcome to be positive (unstable cell) for unit changing of the considered independent variable. Unit changings in the case of continuous or dichotomous discrete variables are straightforward while, in the case of polychotomous discrete variables, are intended in relative terms with respect to a common reference group or class. Negatively correlated variables will produce negative β's and OR limited between 0 and 1; positively correlated variables will result in positive β's and OR greater than 1.

At the same time, the −2LL allows us to compare models obtained by considering different sets of predictors, so that, for example, the significance of the increase in the model fitting produced by including each single landslide factor can be quantitatively assessed. Based

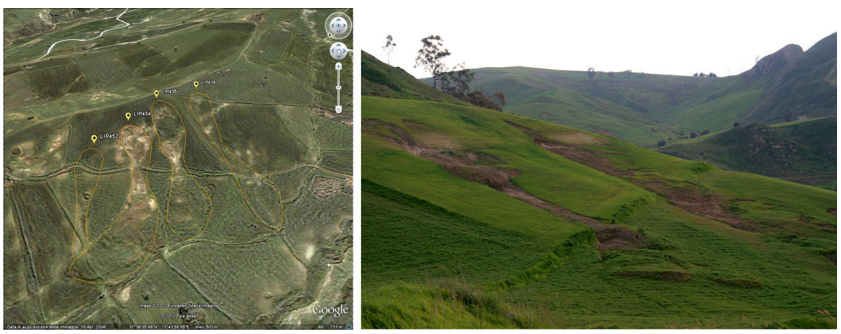

Fig. 3 Remote (*left*: Google Earth) and field (*right*) views of earth-flow landslides in the Tumarrano river basin

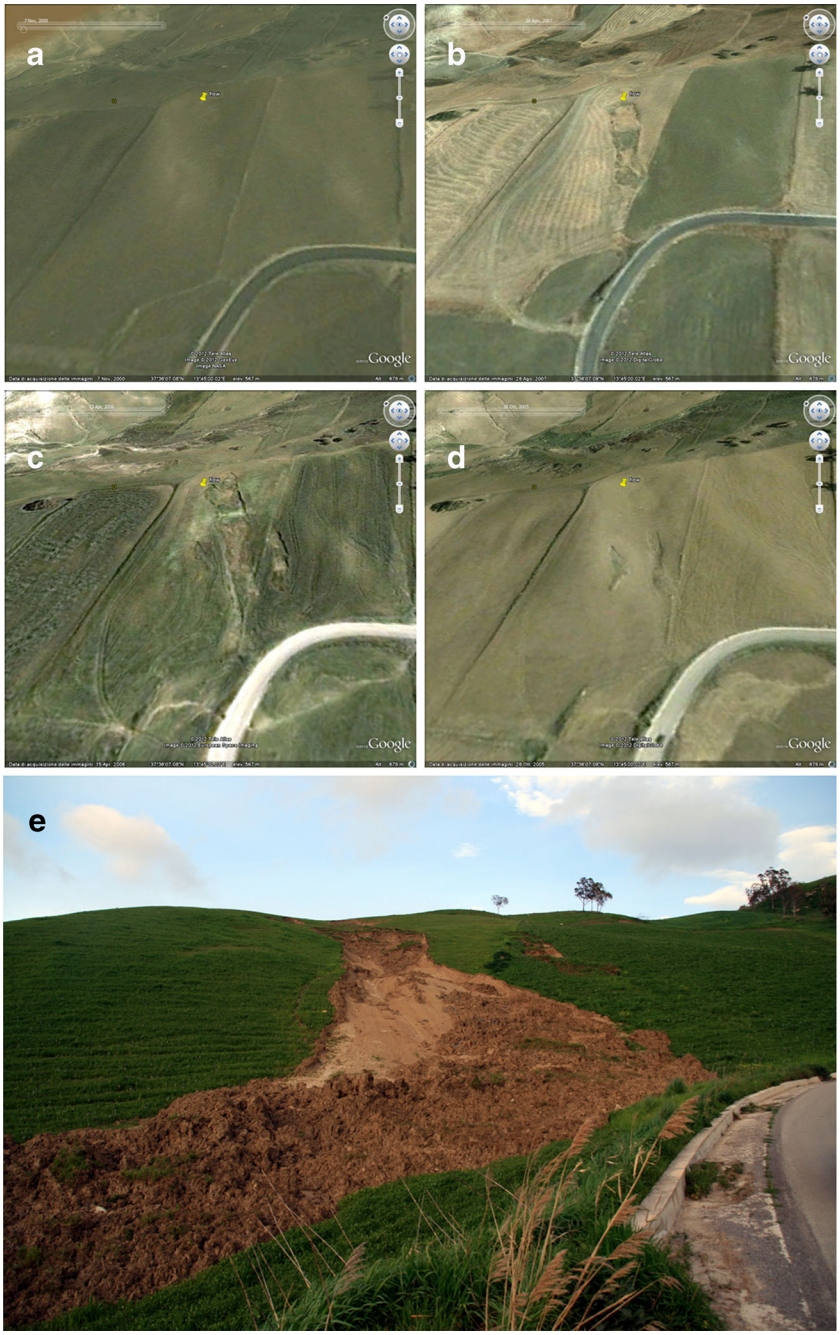

Fig. 4 Example of seasonal reactivation cycles of an earth-flow landslide in the Tumarrano river basin: **a** 2000 (Google Earth™), **b** 2005 (Google Earth™), **c** 2006 (Google Earth™), **d** 2007(Google Earth™), **e** 2009 (from field)

on this approach, logistic regression can be performed following stepwise procedures, which enable us to quantify the importance of a single predictor or combination and select, among a large set of variables, a restricted group made up of only those that significantly increase the performance of the multivariate model. At any step, the most important variable is the one that produces the greatest change in the log-likelihood relative of the model that does not contain it. This procedure describes the *forward selection* scheme in applying multiple logistic regression adopted in this study.

At step o, the fitting of each of the p possible univariate logistic regression models, $L_p^{(o)}$ is compared with the fitting of the "intercept only model," L_o. The first entry, x_{e1}, in the model will be the x_j variable producing the smallest p value for the x^2- test on $G_j^{(o)} = -2(L_o - L_j^{(o)})$. At step 1, the fitting for the model including the intercept and the first entry, x_{e1} is then $L_{e1}^{(1)}$. $p-1$ models, each including the first entry and one of the other remaining predictors, are then prepared and their log-likelihood, $L_{e1j}^{(1)}$, estimated. Again, the variable that minimizes more the p value for the log-likelihood chi-square test on $G_j^{(1)} = -2(L_{e1}^{(1)} - L_{e1j}^{(1)})$ is selected as second entry in the model. The procedure follows in the same manner the final step (m), for which including a jth entry will result in a p value for the log-likelihood chi-square test larger than a threshold significance value, p_E (probability for entry). This threshold, p_E, was set in the following analysis at 0.01. In this research, to perform the forward stepwise logistic regression, an open source software for data mining was used (TANAGRA: Rakotomalala 2005).

Diagnostic areas and mapping units

Diagnostic areas are those sectors spatially or morphodynamically connected to the observed landslides so that their conditions are expected to be similar to those that had characterized the sites where landslides occurred (Rotigliano et al. 2011). Their geoenvironmental conditions are statistically supposed to be the causative factors for landslide occurrence, so that landslide susceptibility can be estimated in terms of similarity of the site conditions of each mapped unit to those of the diagnostic areas. Diagnostic areas can be defined geomorphologically, as pure landforms, or according to morphodynamic and spatial criteria, as neighborhood areas morphodynamically connected to the slopes or sites of past landslides.

It must be mentioned that in a number of papers diagnostic areas simply correspond to the whole landslide polygons, disregarding the morphodynamic heterogeneity of these sectors with respect to past phenomena (Chauan et al. 2010; Das et al. 2011; Felicísimo et al. 2012; Mathew et al. 2009; Rossi et al. 2010). Some researches deal differently with this topic by adopting diagnostic areas that are defined on an analytical basis (Carrara et al. 2008; Nefeslioglu et al. 2008; Rotigliano et al. 2011; Van den Eeckhaut et al. 2009). The most adopted diagnostic areas are selected based on landslide typology: scarps, areas uphill from crowns, and landslide area for rotational slides; source areas and landslide areas for flows; and scarps and areas uphill from crowns for falls. However, a source of subjectivity and ambiguity arises from mapping this kind of diagnostic areas.

In light of the type of landslides considered in this study, which are not strictly dependent on general deep slope geometry but rather on local and surficial hydromorphological features, it was assumed that conditions for new activations could be detected in the detachment areas of flows. Moreover, we decided to test a very simple approach to automatically define these diagnostic areas (Costanzo et al. 2012a, 2012b; Rotigliano et al. 2011): we first generated a landslide identification point (LIP) for each landslide by piking from the 2-m DEM the highest cells along the boundary of the polygons delimiting the landslide area, so that LIPs are positioned along the central sectors of the crown areas (Fig. 2b); we then identify the diagnostic areas in a buffer area of 8 m around the LIPs. This "smoothed buffered" solution exploits the high morphodynamic specificity of the detachment landslide sector (Carrara et al. 2008), which could enable a good discrimination for prediction and allow for a fast extraction of the diagnostic areas from the landslide archive.

In binary logistic regression, the dependent variable or outcome to be predicted has a dichotomic behavior, morphodynamically corresponding to stable or unstable status for a so-called mapping unit: the reference spatial unit for which the model is able to produce a prediction. A large set of mapping units is proposed in literature, mainly subdivided in: grid cells, terrain units, unique condition units, and hydromorphological units (Carrara et al. 1995; Das et al. 2011; Guzzetti et al. 1999; Rotigliano et al. 2011). As a consequence of the criterion adopted in defining the diagnostic areas, the mapping units that were used in this study are 8×8 m cells, whose status was set to unstable or stable depending on the intersection with LIPs.

Controlling factors and independent variables

The first stage in model building was the production of a data matrix, where each row corresponds to an individual case (i.e., a single grid cell or mapping unit), while columnar data show the values of the explanatory and response variables. The data matrix, whose records are the observed cases (i.e., the mapping units or, in this case, grid cell) contain at least $p+1$ fields, which correspond to the information both on the p independents values and on the dependent status. Actually, the number of fields is typically larger due to the need to binarize all the discrete (nominal- and ordinal-scale) variables.

To perform the GIS analysis, raster layers for the outcome (landslides) and all the considered predictor variables were prepared. The selection of the controlling factors that are to be used as independent variables in the logistic regression analysis is typically driven by the following procedure: (1) testing the largest set of geoenvironmental variables that could have statistically significant relationships with slope failures, (2) performing statistical tests so to exclude those variables that result as being not significantly correlated with the dependent (with the exception of those variables that have a high diagnostic morphodynamic meaning), and (3) finally, adopting the most parsimonious, but performing, number of independent variables. The whole sequence must obviously configure acceptable time/money costs for acquisition and processing of the spatial layers of the selected variables. In this sense, a strong constraint is the set of already available variables. Moreover, the predictive performances of each considered factor or variable has to be evaluated considering both its morphodynamic role and the resolution of the available source data.

In light of the main morphodynamic characteristics of the considered landslides, controlling factors were selected in order to directly or indirectly (as proxies) express the conditions that can determine flow initiation on slopes: lithology, hydrology, site and general morphology, and land use. In this study, we exploited a geological map which was specifically prepared for the landslide research and a soil use map, which was derived from the 1:100,000 Corine coverage based on photointerpretation from Landsat 1988 and aerial photos (1:75,000 scale), made available by the Sicilian Region; a field survey was carried out to check and detail the geological and soil use data up to a scale of 1:10,000. As regards the topographic attributes, a detailed DEM (2-m side cell), which was derived from a LIDAR flight, was acquired from the Sicilian Region web GIS databank.

No matter the scale of the source maps from which the geoenvironmental attributes were derived, all the grid layers were structured with a 8-m^2 cell; this was, in fact, the resolution of the mapping unit discretization that was adopted. By processing the source data layers, a set of 17 topographic and two geoenvironmental independent variables was defined (Table 2a, b).

The DEM was processed by using GIS software and tools (ESRI ArcView 3.2 and ArcGIS 9.3, SAGA GIS) to derive the following primary and secondary topographic attributes: aspect, steepness, topographic wetness index, stream power index, and topographic curvatures. Aspect was used for further processing to produce a discrete nominal variable (see below), while the average of the steepness in a neighborhood area of one cell (SLONGB) was computed as a landslide-controlling factor. In this way, more general conditions, rather than local steepness, were included in the model to represent the role of gravitative stress. By using a terrain analysis, ArcView 3.2 script (Topocrop Terrain Indices), topographic wetness index (TWI), and stream power index (SPI) were derived (the contributing area was calculated using the D8 algorithm; O'Callaghan and Mark 1984). These secondary attributes typically express the way in which the surface morphology controls the surface runoff and,

Table 2 **a**: Descriptions of the independent categorical variables **b**: Descriptions of the independent continuous variables

Independent variables			
Categorical variables: binary response [0,1]			
Name: code (source)	Classes	Variable	Count %
Outcropping lithology: LIT (geological map: this study)	Clays	LIT_CLAY	28.845
	Clayey and breccia clays	LIT_CLBRE	44.290
	Clayey sands	LIT_CLYSN	16.457
	Alluvial	LIT_ALL	5.683
	Arenites	LIT_ART	1.849
	Gypsum arenites	LIT_GYART	1.058
	Carbonates	LIT_CARB	0.817
	Marls	LIT_MARL	0.622
	Arenaceous	LIT_ARN	0.247
	Debris	LIT_DBR	0.132
Slope aspect: ASP (derived and reclassified from DEM: SAGA GIS, Olaya 2004)	North	ASP_N	13.016
	North-east	ASP_NE	13.560
	East	ASP_E	11.175
	South-east	ASP_SE	9.624
	South	ASP_S	10.476
	South-west	ASP_SW	14.791
	West	ASP_W	14.001
	North-west	ASP_NW	13.356
Curvature classification: CCL (derived from DEM: SAGA GIS, Olaya 2004)	Convex/concave	CCL_CXCC	34.907
	Planar/concave	CCL_PCC	31.795
	Concave/convex	CCL_CCXC	17.799
	Planar/planar	CCL_PP	15.243
	Concave/planar	CCL_CCP	0.105
	Convex/convex	CCL_CXCX	0.079
	Planar/convex	CCL_PCX	0.069
	Convex/planar	CCL_CXP	0.002
Landform classification: LCL (derived from DEM: ArcView 3.2+topographic position index, Jenness 2006)	Upper slopes, mesas	LCL_UPPSLO	49.344
	Local ridges/hills in valleys	LCL_LOCRID	9.446
	Canyons, deeply lincised streams	LCL_CANDEE	8.363
	Midslope drainages, shallow valleys	LCL_MIDDRAIN	7.494
	Midslope Rridges, small hills in plains	LCL_MIDRID	6.722
	Open slopes	LCL_OPEN	6.445
	Plains small	LCL_PLASMA	5.986
	U-shaped Vvalleys	LCL_USHAPE	5.603
	Upland drainages, headwaters	LCL_UPDRAIN	0.453
	Mountain tops, high Rridges	LCL_MOUNTOP	0.144
Land use (Corine 2006 project)	Non irrigated arable lands	USE_211	86.786
	Fruit tree and berry plantatations	USE_222	0.628
	Olive trees	USE_223	2.692
	Pastures	USE_231	1.201
	Coniferous forest	USE_312	3.875

Table 2 (continued)

Independent variables			
	Burnt areas	USE_334	0.594
	Natural grasslands	USE_321	0.201
	Sclerophyllus vegetation	USE_323	3.817
	Beaches, dunes, and sand plains	USE_331	0.206
Continuous variables			
Name	Description	DEM processing GIS- tools	
HEIGHT	Elevation	SAGA GIS	
SLOPENGB	Neighborood steepness	SAGA GIS	
TWI	Topographic wetness lindex	ArcvView 3.2+Topocrop Terrain Indices	
SLOPETWI	Slope-TWI	ArcvView 3.2+Topocrop Terrain Indices	
SPI	Stream power lindex	ArcvView 3.2+Topocrop Terrain Indices	
SLOPESPI	Slope_SPI	ArcvView 3.2+Topocrop Terrain Indices	
8PROFCONC	Local profile concave curvature	SAGA GIS	
8PROFCONV	Local profile convex curvature	SAGA GIS	
8PLANCONV	Local plan convex curvature	SAGA GIS	
8PLANCONC	Local plan concave curvature	SAGA GIS	
16PROFCONC	Large profile concave curvature	SAGA GIS	
16PROFCONV	Large profile convex curvature	SAGA GIS	
16PLANCONV	Large plan convex curvature	SAGA GIS	
16PLANCONC	Large plan concave curvature	SAGA GIS	

potentially, infiltration and water erosion phenomena, respectively (Wilson and Gallant 2000). Thus, as the drainage network is characterized by the highest values of contributing area, TWI and SPI typically have their highest values along the high and low order drainage axes, respectively. This produces a saturation of the scale of these variables, responsible for a lower discrimination between the cells onto the slopes (which are the ones from which landslides trigger). A further processing of these variables was performed, and TWISLO and SPISLO variables were also computed by dividing TWI and SPI values, respectively, for their standard deviation evaluated for a neighborhood of two cells; the latter, in fact, ranges from minimum, along the streams, to maximum, away from streams on slopes, where both TWI and SPI values are lower but more constant. Topographic curvatures were also derived both considering a local (one cell=8 m) and a large (two cells=16 m) curvature calculation. Eight curvature variables were so derived, by combining planar or profile and concave or convex shapes, for the two 8-m and 16-m curvatures: 8PLANCONC, 8PLANCONV, 8PROFCONC, 8PROFCONV, 16PLANCONC, 16PLANCONV, 16PROFCONC, and16PROFCONV were so derived. The altitude (HEIGHT) of each cell was also used as a proxy variable to represent possible rainfall or climatic variations inside the basin.

From the geological map, a grid layer of the outcropping lithology (LIT) was prepared, assuming that each of the ten lithology potentially is responsible for a different morphodynamic response. The Corine 2006 coverage was converted in a grid file of soil use (USE) by using the third level full Corine legend. Aspect (ASP), curvature classification (CCL), and landform classification (LCL) were derived by processing the DEM with topographic analysis tools. Aspect was defined by partitioning the whole 360° range into eight 45° interval classes. Landform classification was derived by using a freeware ArcView extension tool (Jenness 2006) that compares small and large neighborhood topographic position index (TPI) computed for each cell. The TPI values reflect the difference between the elevation of the considered cell and the average elevation in the neighborhood area. To compute the TPI, the inner and the outer neighborhood areas were set to 400 and 800 m, respectively. Ten landform classes are obtained allowing us to assign the morphological conditions (position and shape) to each cell. Finally, curvature classification was obtained by processing the DEM exploiting a terrain analysis module (Morphometry) of SAGA GIS (Olaya 2004).

All the discrete variables were binarized before being included in the logistic regression-based model-building procedure. Logistic regression requires a dataset composed of a near-balanced number of positive (unstable) and negative (stable) cases (Atkinson and Massari 1998; Bai et al. 2010; Frattini et al. 2010; Nefeslioglu et al. 2008; Süzen and Doyuran 2004; Van Den Eeckhaut et al. 2009). When using grid cell-based models, which exploit very small cell size so as to increase the spatial resolution of factors and diagnostic areas, positive cases are typically fewer than negatives; in fact, the diagnostic areas include only a few more

neighboring cells around the LIPs, while all the stable areas (outside the landslide areas) correspond to hundreds of thousands of stable cells, from which a negative subset is randomly extracted. Logistic regression is then performed only on the balanced positive/negative subset, which means to take into consideration only a very small percentage of the studied area! This could reduce the robustness of the model, as the regressed logistic equation will depend on the particular set of selected stable cells. By performing more than one random extraction of negatives cases, different equations could arise. Furthermore, each of the models could be affected by overfitting, as it will work very well inside a cluster of the hyperspace of the p predictors, whose shape and dimension will depend on the characteristics of the actual worked cells.

Likewise, in the present research, because of the very low number of positive cases or unstable cells (760), a balanced model accounts only for a very poor portion of the whole studied area (1,520 over 1,213,092 total cells). That would mean training the susceptibility model on just 0.124 % of the whole basin! To explore the effects produced by enlarging the area on which the model is trained, a suite of models was prepared by differently merging the set of 760 LIPs and randomly extracted subsets of stable cells. In order to face the problem of sizing and selecting the landslide-free cells, a multiple balanced-suite randomly extraction was used in this research.

A suite of 1,520 counts models was prepared by merging the 760 unstable cells with 16 different randomly selected subsets of 760 stable cells: all the unstable 760 LIPs were systematically included in each model, together with an equal number of stable cells which were randomly extracted from the set of the stable cells. It is important to note that differently from the 760 LIPs, which are systematically included, each unstable subset was included in only one model. In this way, a total number of [760+(760*16)]=1,920 cells, corresponding to around the 1 % of the whole investigated area, was included in the suite of models.

Validation

To estimate the performance of a susceptibility model, different stages of the model building procedure are to be taken into consideration. Particularly, *model fitting*, *prediction skill*, and *robustness* are among the main performance characteristics which must be quantitatively estimated (Carrara et al. 2008; Frattini et al. 2010; Guzzetti et al. 2006; Rossi et al. 2010).

The model fitting expresses the *adequacy* and *reliability* with which the model classifies the known phenomena (i.e., the positive and negative cases on which the *maximum likelihood* method has worked in estimating the ' coefficients). Model fitting was evaluated for each model by computing the statistic −2LL: the larger the negative log-likelihood, the better the fit of the model. The logistic regression component of the software TANAGRA also provides the results of the model chi-square test, which allows for assessing the global significance of the regression coefficients. The significance was also evaluated individually for each independent variable incorporated in the model by means of the Wald test. Together with the confusion matrices, which were used in this research, other alternative methods can be adopted to estimate the model fitting, such as those quoted in Frattini et al. (2010) and Guzzetti et al. (2006). The model fitting was also evaluated by exploiting two pseudo-R^2 statistics: the McFadden R^2 and the Nagelkerke R^2. The first is defined as $1-(L_{MODEL}/L_{INTERCEPT})$ being confined between 0 and 1. As a rule of thumb (Mc Fadden

Table 3 Performances of the model suite: error rate, −−2LL test, McFadden and Nagelkerke pseudo -R^2, and AUCs of the ROC curves

Model suite																		
	M01	M02	M03	M04	M05	M06	M07	M08	M09	M010	M011	M012	M013	M014	M015	M016	Average std. dev.VERAGE STD.DEV.	
Error rate	0.2439	0.2272	0.2316	0.2395	0.2596	0.2281	0.2307	0.2228	0.2368	0.2351	0.2430	0.2325	0.2219	0.2298	0.2307	0.2439	0.2348	0.010
−−2LL intercept	1,572.044	1,572.044	1,572.044	1,572.044	1,572.044	1,572.044	1,572.044	1,572.044	1,572.044	1,572.044	1,572.044	1,572.044	1,572.044	1,572.044	1,572.044	1,572.044	1,572.04	0.00
−−2LL model	1,131.535	1,133.699	1,172.383	1,159.81	1,187.809	1,101.785	1,138.118	1,083.559	1,142.463	1,110.029	1,149.155	1,108.188	1,116.559	1,138.753	1,152.826	1,156.830	1,136.47	27.43
ChiHJ square	440.509	438.345	399.661	412.234	384.235	470.259	433.926	488.485	429.581	462.015	422.889	463.856	455.485	433.291	419.218	415.214	435.58	27.43
d.f.	15	11	15	12	13	15	12	12	12	13	10	11	14	11	15	12	12.7	1.7
P (>chi square)	0.0000	0.0000	0.0000	0.0000	0.0000	0.0000	0.0000	0.0000	0.0000	0.0000	0.0000	0.0000	0.0000	0.0000	0.0000	0.0000	0.0000	0.0000
McFaden'S's R^2	0.2802	0.2788	0.2542	0.2622	0.2444	0.2991	0.2760	0.3107	0.2733	0.2939	0.2690	0.2951	0.2897	0.2756	0.2667	0.2641	0.2771	0.0174
Nagelkerke's'S R^2	0.4292	0.4275	0.3960	0.4064	0.3832	0.4526	0.4239	0.4667	0.4204	0.4462	0.4150	0.4476	0.4411	0.4234	0.4121	0.4088	0.4250	0.0220
AUC ROC (known LIPs)	0.841	0.840	0.834	0.831	0.820	0.852	0.838	0.853	0.837	0.850	0.832	0.844	0.847	0.842	0.835	0.829	0.839	0.009
AUC ROC (unknown LIPs)	0.824	0.830	0.825	0.841	0.828	0.792	0.826	0.789	0.811	0.820	0.805	0.785	0.817	0.834	0.822	0.828	0.817	0.017

1979), values between 0.2 and 0.4 attest for excellent fit. Nagelkerke R^2 is a corrected pseudo-R^2 statistics, ranging from 0 to 1 (Nagelkerke 1991). At the same time, mathematical or statistical evaluation on how well the predictors describe the known phenomena must be coherent with a geomorphologic interpretation of the results (adequacy), so as to give sense to the overall relationships between landslides and factors.

The prediction skill of the model, which corresponds to its ability to predict the unknown stable and unstable cases, can be obtained (as was done in this study) by randomly extracting a subset of cells from the initial dataset before proceeding in regressing the model. In some other cases, available temporal or spatial partitioned landslide inventories can be exploited.

The accuracy of logistic regression in modeling landslide susceptibility of the study area was evaluated by drawing, for each model, the receiver operating characteristic (ROC) curves (Goodenough et al. 1974; Lasko et al. 2005) and by computing the values of the area under the ROC curve (AUC; Hanley and McNeil 1982). A ROC curve plots true positive rate TP (sensitivity) against false positive rate FP (1−specificity), for all possible cutoff values; sensitivity is computed as the fraction of unstable cells that were correctly classified as susceptible, while specificity is derived from the fraction of stable cells that were correctly classified as nonsusceptible. The closer the ROC curve to the upper left corner (AUC=1), the higher the predictive performance of the model; a perfect discrimination between positive and negative cases produces an AUC value equal to 1, while a value close to 0.5 indicates inaccuracy in the model (Akgün and Türk 2011; Fawcett 2006; Nandi and Shakoor 2009; Reineking and Schröder 2006). In relation to the computed AUC value, Hosmer and Lemeshow (2000) classify a predictive performance as acceptable (AUC>0.7), excellent (AUC>0.8), or outstanding (AUC>0.9). ROC curves were drawn both for the validation (test) and calibration (training) cells, in order to evaluate the predictive performances of the models and to further investigate their fit to the training observations (model fitting); moreover, the difference between apparent accuracy (on training data) and validated accuracy (on test data) indicates the amount of overfitting (Märker et al. 2011).

Once a balanced model was prepared, a 75 % random proportional splitting of the data was further applied to extract the calibration cells subset, which was then used for the logistic regression. The 25 % percent not used for calibration was finally exploited for validating the model and estimating its prediction skill.

Finally, the robustness of the model depends on its invariance with respect to small changes both in the input variables and in the model building procedure. The robustness of the models is typically evaluated by preparing suite or ensemble of models (e.g., Guzzetti et al. 2006; Van Den Eeckhaut et al. 2009), obtained by randomly extracting multiple, but not overlapping, subsets of the whole investigated area and comparing the regressed models in terms of selected factors, adequacy, *precision*, and *accuracy*.

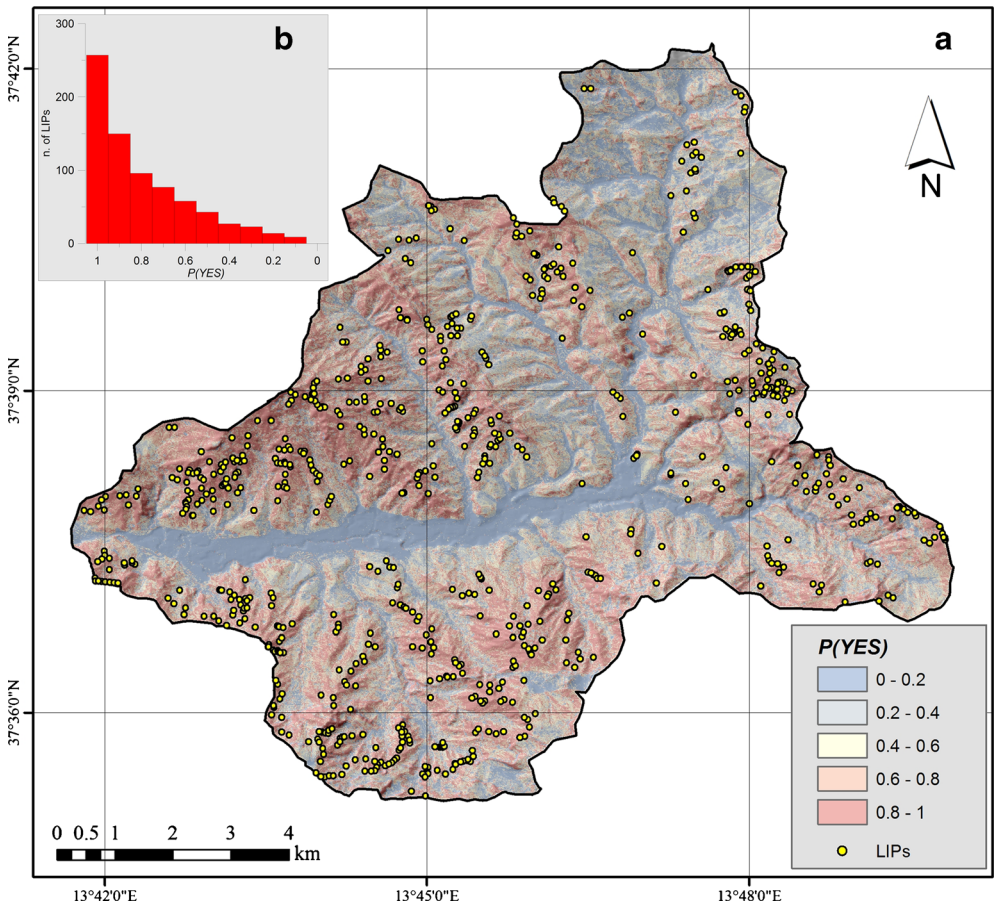

Fig. 5 **a** Earth-flow susceptibility map for the best model (M13). **b** Frequency distribution of positives (LIPs) on the probability (susceptibility) classes

Results

On the whole, the model suite produces good fittings (Table 3) which are characterized by a mean error rate of 0.235 (std. dev.=0.01), Mc Fadden R^2=0.28, and AUC values higher than 0.8. On the basis of a multicriteria selection (best Nagelkerke and Mc Fadden R^2, maximum sum and minimum difference between training and test ROC curves AUCs, and minimum error rate), the model M13 was adopted as the best and applied to produce the susceptibility map (Fig. 5). The confusion matrix (Table 4) attests for recall and 1−precision larger for "NO" than "YES," with differences of 0.0413 and 0.0195, respectively, while all the pseudo-R^2 statistics attest for excellent fitting as well.

AUC values for both the two (known and unknown LIPs) ROC curves (Fig. 6) are excellent (AUC>0.8) with the exception of models 6, 8, and 12, for which it is, however, largely acceptable (AUC>0.75). The stability of the AUCs is higher for the training (std. dev.=0.009) than for the test dataset (std. dev.=0.017).

As regards the predictors (Table 5), a first group of six variables was selected more than 15 times with a very high mean rank order (i.e., the iteration of the forward selection procedure, in which they are extracted), which is less than 8: SLOPENGB was systematically extracted as the first predictor, with a positive coefficient; 16PROF and 8PLAN curvatures, showing negative and positive coefficients, respectively, with a mean rank R of less than 4, with the exception of 16PROFCONC; and LIT_CLAYS, with a positive coefficient and a mean rank of less than 6, is selected for 15/16. A second group includes four variables that were selected less than 16 times but more than 50 % (8) times: LCL_MIDDRAIN and LCL_MIDRID, with negative coefficients, and LCL_LOCRID and LCL_CANDEE, with positive coefficients; high mean ranks characterize the LCL selected classes. Finally, a third group includes the nine variables that were selected at least four times (25 %), with middle–high rank orders (between 6 and 12): LIT_ALL, 8PROFCONV, TWI, SLOPETWI, and LCL_UPPSLO, with negative coefficients, and ASP_W, CCL_PP, 16PLANCONC, and LCL_PLASM, with positive coefficients. With the exception of LIT_ALL, the selected variables produced high (>95 %) significance Wald tests. All the selected variables were regressed with congruent coefficients (always positive or negative, with the exception of LCL_UPPSLO) and quite constant ranks.

Discussion and concluding remarks

The research whose results are here presented deals with two main topics: adopting automatically generated point representation for landslides (the LIPs) and defining simplified procedures to assess the robustness of grid cell models based on logistic regression. In particular, a procedure is proposed for verifying the robustness of logistic regression landslide (earth-flow) susceptibility models with respect to the specific locations of the stable cells which have to be included in the regressed subset to balance those which are stable. Without taking into consideration the whole area, it is, in fact, possible to work on a limited suite of models to check for large variations in the results, when changing the stable cases. At the same time, the possibility of exploiting LIPs to select positive (unstable) cases was explored.

In spite of the striking criticism which arises when selecting only a very limited subset of the mapped areas, a number of papers, which exploit logistic regression methods to produce grid cell susceptibility models, optimizes very sophisticated statistic procedures but disregards the real spatial representativeness of the fitted models; in these studies, models are trained solely on very limited part of the mapped basins, which typically stretch for hundreds of square kilometers, without verifying if changes in the random extraction of negative

Table 4 Confusion matrix for the model suite

TP	FN	FP	TN	Yes	No	TOT	Error rate	Recall		1−precision		Suite
								Yes	No	Yes	No	
422	149	129	440	571	569	1,140	0.24386	0.7391	0.7733	0.2341	0.2530	M01
425	146	113	456	571	569	1,140	0.22719	0.7443	0.8014	0.2100	0.2425	M02
425	146	118	451	571	569	1,140	0.23158	0.7443	0.7926	0.2173	0.2446	M03
426	145	128	441	571	569	1,140	0.23947	0.7461	0.7750	0.2310	0.2474	M04
420	151	145	424	571	569	1,140	0.25965	0.7356	0.7452	0.2566	0.2626	M05
435	136	124	445	571	569	1,140	0.22807	0.7618	0.7821	0.2218	0.2341	M06
433	138	125	444	571	569	1,140	0.23070	0.7583	0.7803	0.2240	0.2371	M07
422	149	105	464	571	569	1,140	0.22281	0.7391	0.8155	0.1992	0.2431	M08
420	151	119	450	571	569	1,140	0.23684	0.7356	0.7909	0.2208	0.2512	M09
428	143	125	444	571	569	1,140	0.23509	0.7496	0.7803	0.2260	0.2436	M10
431	140	137	432	571	569	1,140	0.24298	0.7548	0.7592	0.2412	0.2448	M11
434	137	128	441	571	569	1,140	0.23246	0.7601	0.7750	0.2278	0.2370	M12
431	140	113	456	571	569	1,140	0.22193	0.7548	0.8014	0.2077	0.2349	M13
424	147	115	454	571	569	1,140	0.22982	0.7426	0.7979	0.2134	0.2446	M14
425	146	117	452	571	569	1,140	0.23070	0.7443	0.7944	0.2159	0.2441	M15
413	158	120	449	571	569	1,140	0.24386	0.7233	0.7891	0.2251	0.2603	M16
425.9	145.1	122.6	446.4	571	569	1,140	0.23481	0.7458	0.7846	0.2233	0.2453	Mean
5.9	5.9	9.8	9.8	0	0	0	0.00953	0.0104	0.0173	0.0138	0.0082	STDV

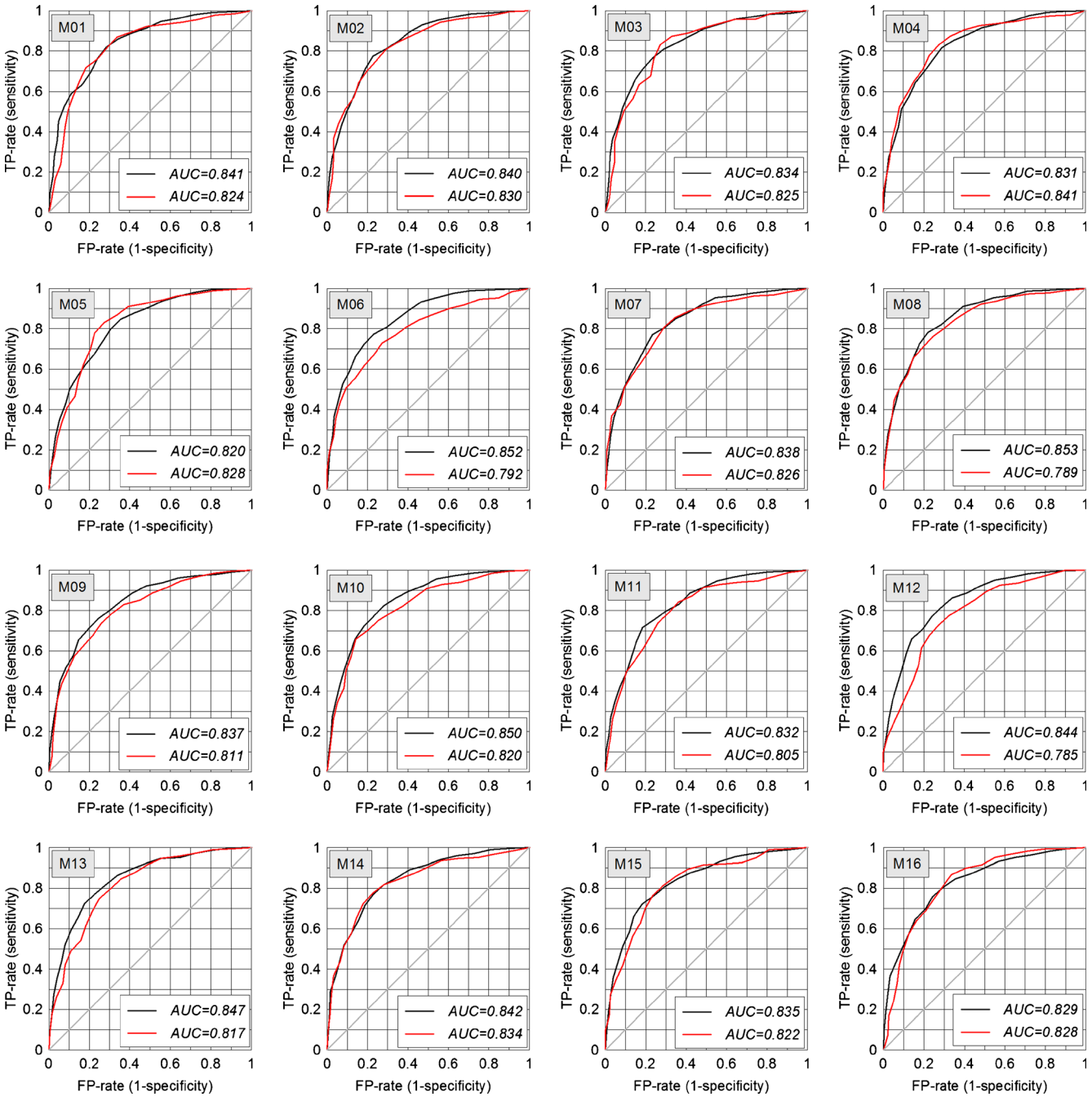

Fig. 6 ROC curves for the 16 landslide susceptibility models (see also Table 3)

cases result in modifying the selected factors or their regression coefficients (Akgün 2012; Chauan et al. 2010; Erener and Düzgün 2010; Mathew et al. 2009; Nefeslioglu et al. 2008; Ohlmacher and Davis 2003; Süzen and Doyuran 2004). At the same time, some other papers in literature deal with the estimation of robustness in terms of stability of the statistical procedure, disregarding the problem of the geologic representativeness of the subset on which regression is applied (e.g., Carrara et al. 2008; Vorpahl et al. 2012), using totally boot strapping-based procedures.

The strategy here adopted seems to be adequate enough to apply logistic regression, which requires a balanced sizing of the worked dataset, without losing the connection between reliability and accuracy of the susceptibility model and its real spatial representativeness. In fact, though about just 1 % of the whole area was included in the worked dataset, comparing the selected factors (ranking and coefficients) and performances of each of a suite of 16 balanced datasets, the robustness of the regressed model was evaluated. The good stability of the results suggested that there is need to increase the number of models in the suite for the investigated area. Otherwise, in case of higher variability, automatic model building procedure could be implemented to consider a larger fraction of the whole area (in this case, 160 models would have been required to reach up to 10 % of the area). Performing multiextraction of different negative subsets allows us to prepare

Table 5 Predictors selected by the forward logistic regression of the model suite

						R (model suite)																	
Predictors	Coef.	Std-dev	Wald	Signif	Odds	*R*	FREQ	M1	M2	M3	M4	M5	M6	M7	M8	M9	M10	M11	M12	M13	M14	M15	M16
SLOPENGB	0.097	0.0293	46.5	0.0159	1.1024	1.0	16	1	1	1	1	1	1	1	1	1	1	1	1	1	1	1	1
16PROFCONV	−1.553	0.2125	65.1	0.0000	0.2161	2.7	16	2	4	2	2	3	2	2	4	2	2	2	2	5	2	5	2
8PLANCONC	1.431	0.2237	59.5	0.0000	4.2788	3.4	16	3	3	3	5	5	4	3	3	3	3	3	3	3	4	4	3
8PLANCONV	1.296	0.2385	48.9	0.0000	3.7601	3.6	16	4	2	4	4	4	3	4	2	4	4	4	4	2	5	3	4
16PROFCONC	−0.710	0.2000	25.2	0.0006	0.5009	7.2	16	10	9	6	6	10	5	5	5	7	5	5	5	10	7	15	5
LIT_CLAYS	0.616	0.1340	17.2	0.0019	1.8665	5.9	15	6	6	5	10	2	10	6	6		6	6	6	6	6	2	6
LCL_MIDDRAIN	1.100	0.3179	20.1	0.0001	3.1740	7.5	13	9	7	7	8		6		7	6	10		8	9	3	10	9
LCL_LOCRID	−1.237	0.3133	11.7	0.0033	0.3025	9.8	13		11		11	6	9	11	12	10	13	7	7	12	11		7
LCL_CANDEE	0.888	0.2978	14.3	0.0021	2.5415	8.9	11	14	8	8	7		7		8	8	10			8		8	12
LCL_MIDRID	−1.370	0.2558	13.7	0.0009	0.2613	8.1	8	7				11		7	9		7	8			8		8
ASP_W	0.655	0.0605	10.2	0.0019	1.9288	11.0	7	11		9			14		10					11		12	10
16PLANCONC	0.715	0.1211	11.6	0.0018	2.0578	6.7	6		5		3			9		9				7		7	
8PROFCONV	−0.391	0.1236	11.2	0.0041	0.6803	6.8	6					7	8			5				4		6	11
CCL_(P/P)	0.566	0.0387	9.2	0.0029	1.7630	9.4	5	8										10	10		10	9	
LITO_ALL	−5.116	5.5536	5.1	0.2067	0.0584	10.6	5		10			8	15		11				9				
SLOPETWI	−0.006	0.0009	9.6	0.0033	0.9936	11.6	5					9	13				11		11	14			
TWI	−0.630	0.2678	11.5	0.0027	0.5459	10.0	4	5			12			10						13			
LCL_PLASMA	1.186	0.3575	15.5	0.0013	3.4350	10.3	4			10			11				9					11	
LCL_UPPSLO	−0.202	0.6083	11.3	0.0013	0.9604	11.5	4			13		12		12				9					
8PROFCONC	0.424	0.0534	11.8	0.0013	1.5297	8.7	3				9			8							9		
CCL_(CX/CC)	−0.550	0.0208	10.5	0.0013	0.5768	11.5	2			11			12										
SLOPESPI	−0.160	0.0582	11.8	0.0013	0.8527	12.0	2	12		12													
HEIGHT	0.002	0.0001	8.4	0.0039	1.0021	13.0	2									12						14	
LIT_CLAYSAN	−0.807	0.0000	13.0	0.0003	0.4464	11.0	1									11							
ASP_NE	−0.677	0.0000	8.3	0.0040	0.5082	12.0	1										12						
USE_211	0.802	0.0000	11.3	0.0008	2.2306	13.0	1										13						
USE_231	−2.355	0.0000	5.4	0.0203	0.0949	13.0	1										13						
SPI	0.428	0.0000	13.6	0.0002	1.5342	13.0	1	13															
LCL_UPPDRAIN	15.449	0.0000	0.0	0.9820	5123150	14.0	1			14													
ASP_SW	0.539	0.0000	7.4	0.0065	1.7148	15.0	1	15															

suites of partially overlapped models, which share only positive cases. Boot strapping-based procedures can be then applied on each single model to assess their reliability. In few papers, similar multiselection procedures are applied, but for producing grid cell models based on canonical discriminant analysis, using unbalanced (1/5) extraction of positive and negative, respectively (e.g., Van den Eeckhaut et al. 2009).

The problem of sizing the dataset should be never overlooked when exploiting logistic regression for modeling landslide susceptibility. Model suite generation together with forward selection procedure is one of the possible tools to cope with intrinsic limits of logistic regression. In this research, the procedure adopted in building the earth-flow susceptibility model allowed us to obtain 16 performing models, whose fitting and prediction skill resulted in being very stable, so that these can be considered as not dependent on the particular locations of the extracted unstable cells. The robustness of the procedure was tested both in terms of selected variables and predictive performances of the suite of models.

Particularly, the forward logistic regression procedure selected 10 predictors eight times out of 16, while a subset of nine predictors was selected a number of times between four and seven, and 51 predictors at least one time. Also, for each of the selected variables, the regression coefficients obtained from the suite of models have coherent signs and very stable values. The number of predictors selected for each model of the suite is also quite similar (12.7; std. dev.=1.3). It is generally verified that the more frequently a predictor is selected, the higher the rank order in the list of controlling factors, for which it is singled out. At the same time, very small differences were observed for each model between training and test ROC curves, attesting for negligible overfitting.

As regards the use of LIPs, these have demonstrated to be sensitive in indicating homogeneous geoenvironmental conditions and specific enough to produce a low number false positives, whatever the selected (out of 16) group of negatives. At the same time, using LIPs represents a good compromise between adequateness and objectivity: these are, in fact, automatically generated by picking the cells at the top of the depletion zones which are the ones that, according to basic morphodynamic models, typically show site conditions similar to those responsible for past activations (Carrara et al. 2008; Nefeslioglu et al. 2008; Rotigliano et al. 2011). The use of a single point to represent a diagnostic area reduces problems of spatial autocorrelation (Van den Eeckhaut et al. 2009), while the automatic generation of the LIPs speeds up the modeling procedure and avoids the subjectivity of the operator.

The main controlling factors for earthflow landslides in the study area are: topography (steepness and curvatures), outcropping lithology (clays), and landform classification (midslope drainages, canyons, local, and midslope ridges). As expected, the probability of having unstable conditions is positively correlated with the mean steepness in the neighborhood of the cells. No matter the sign, topographic local plan curvatures, and large profile curvatures showed positive and negative correlations, respectively. This seems to indicate these curvatures as good predictors because they express the role of mechanical stresses (connected to the local shape of the topographic surface) rather than indicating convergences/divergences of runoff. Concavities and convexities showed, on average, very similar positive coefficients for local plan curvature. As regards the large profile curvature, convexities influence (decrease) the odds of unstable cells much more than concavities. Ridges are not the sites for unstable cells, while these are much more likely on the slopes of midslope drainages and canyons. This means that earth-flow crowns are far downhill from the head of the slopes, where in some cases, rotational slides are recognized. Westward slope aspect is a positive condition for landslides, while, as expected, clayey outcropping lithology is a very important condition for determining unstable conditions. Alluvial deposits, on the contrary, seem to be stable, even if this predictor showed a very low significance in the Wald test. At the same time, these relationships could be due to the fact that alluvial deposits outcrop down on valley floor, where landslides are not possible due to topographic conditions. Surprisingly, both TWI and SLOPETWI are negatively correlated with the odds of unstable cells, which could be due to the prevalence of the steepness control in landsliding (high TWI occurs on low steepness). Slope aspect and curvature classification were involved in the models with only one class, among the most selected predictors. Soil use resulted to be almost useless in predicting unstable cells.

According to the model, clayey, short, and steep slopes are those which produce high susceptibility conditions, while, where slopes decline and enlarge, earth flows are less likely to occur. At the same time, the southwestern-facing slopes of the shorter subbasins, close to the confluence into the Platani river, are the sites for the highest probability for new activations.

In spite of the need for landslide hazard studies to support projects for the strengthening of transportation infrastructure, which are mandatory for the socioeconomic development of inner areas of southern Italy, the Tumarrano river basin was uncovered by landslide studies before this research. Furthermore, the study area is highly representative of the geologic and geomorphologic setting of a large sector of western-southern Sicily, which makes the obtained results of importance as a reference test.

Acknowledgments

The findings and discussion of this research were carried out in accordance with the bilateral agreements between the University of Palermo and the University of Granada supporting an international PhD program. All authors have commonly shared all parts of the paper. This research was supported by the project SUFRA_SICILIA funded by the Department of Earth and Sea Sciences of University of Palermo and the "Assessorato Regionale Territorio e Ambiente della Regione Sicilia". Clare Hampton has linguistically edited the final version of this text. Authors wish to thank two anonymous referees who have allowed us to improve the quality of the paper.

References

Akgün A (2012) A comparison of landslide susceptibility maps produced by logistic regression, multi-criteria decision, and likelihood ratio methods: a case study at İzmir, Turkey. Landslides 9:93–106

Akgün A, Türk N (2011) Mapping erosion susceptibility by a multivariate statistical method: a case study from the Ayvalık region, NW Turkey. ComputGeosci 37:1515–1524

Aleotti P, Chowdhury R (1999) Landslide hazard assessment: summary review and new perspectives. Bull Eng Geol Env 58:21–44

Atkinson PM, Massari R (1998) Generalised linear modeling of susceptibility to landsliding in the central Apennines, Italy. Comput Geosci 24:373–385

Ayalew L, Yamagishi H (2005) The application of GIS-based logistic regression for landslide susceptibility mapping in the Kakuda-Yahiko Mountains, Central Japan. Geomorphology 65:15–31

Baeza C, Corominas J (2001) Assessment of shallow landslide susceptibility by means of multivariate statistical techniques. Earth Surf Proc Land 26:1251–1263

Bai SB, Wang J, Lü GN, Zhou PG, Hou SS, Xu SN (2010) GIS-based logistic regression for landslide susceptibility mapping of the Zhongxian segment in the Three Gorges area, China. Geomorphology 115:23–31

Brenning A (2005) Spatial prediction models for landslide hazards: review, comparison and evaluation. Nat Hazard Sys 5:853–862
Can T, Nefeslioglu HA, GokceogluC SH, Duman TY (2005) Susceptibility assessments of shallow earthflows triggered by heavy rainfall at three catchments by logistic regression analysis. Geomorphology 72:250–271
Carrara A (1983) Multivariate models for landslide hazard evaluation. Math Geol 15:403–426
Carrara A, Cardinali M, Guzzetti F (1995) GIS technology in mapping landslide hazard. In: Carrara A, Guzzetti F (eds) Geographical information systems in assessing natural hazards. Kluwer, Dordrecht, pp 135–175
Carrara A, Crosta G, Frattini P (2008) Comparing models of debris-flow susceptibility in the alpine environment. Geomorphology 94:353–378
Chacón J, Corominas J (2003) Special issue on "landslides and GIS". Nat Hazards 30:263–512
Chacón J, Irigaray C, Férnandez T, El Hamdouni R (2006) Engineering geology maps: landslides and geographical information systems. Bull Eng Geol Environ 65:341–411
Chauan S, Sharma M, Arora M (2010) Landslide susceptibility zonation of the Chamoli region, Garhwal Himalayas, using logistic regression model. Landslides 7:411–423
Clerici A, Perego S, Tellini C, Vescovi P (2010) Landslide failure and runout susceptibility in the upper T. Ceno valley (Northern Apennines, Italy). Nat Hazards 52:1–29
Conforti M, Robustelli G, Muto F, Critelli S (2012) Application and validation of bivariate GIS-based landslide susceptibility assessment for the Vitravo river catchment (Calabria, south Italy). Nat Hazards 61:127–141
Conoscenti C, Di Maggio C, Rotigliano E (2008) GIS analysis to assess landslide susceptibility in a fluvial basin of NW Sicily (Italy). Geomorphology 94:325–339
Costanzo D, Cappadonia C, Conoscenti C, Rotigliano E (2012a) Exporting a Google Earth™ aided earth-flow susceptibility model: a test in central Sicily. Nat Hazards 61:103–114
Costanzo D, Rotigliano E, Irigaray C, Jiménez-Perálvarez JD, Chacón J (2012b) Factors selection in landslide susceptibility modeling at large scale following the GIS-matrix method: application to the river Beiro basin (Spain). Nat Hazard Sys 12:327–340
Dai FC, Lee CF (2002) Landslide characteristics and slope instability modeling using GIS, Landau Island, Hong Kong. Geomorphology 42:213–228
Das I, Stein A, Kerle N, Dadhwal VK (2011) Probabilistic landslide hazard assessment using homogeneous susceptible units (HSU) along a national highway corridor in the northern Himalayas, India. Landslides 8:293–308
Davis JC, Ohlmacher GC (2002) Landslide hazard prediction using generalized logistic regression. Proceedings of IAMG 2002, Berlin, pp 501–506
Erener A, Düzgün HSB (2010) Improvement of statistical landslide susceptibility mapping by using spatial and global regression methods in the case of More and Romsdal (Norway). Landslides 7:55–68
Ermini L, Catani F, Casagli N (2005) Artificial neural networks applied to landslide susceptibility assessment. Geomorphology 66:327–343
Fawcett T (2006) An introduction to ROC analysis. Pattern Recogn Lett 27:861–874
Felicísimo A, Cuartero A, Remondo J, Quirós E (2012) Mapping landslide susceptibility with logistic regression, multiple adaptive regression splines, classification and regression trees, and maximum entropy methods: a comparative study. Landslides. doi:10.1007/s10346-012-0320-1
Frattini P, Crosta G, Carrara A (2010) Techniques for evaluating the performance of landslide susceptibility models. Eng Geol 111:62–72
Goodenough DJ, Rossmann K, Lusted LB (1974) Radiographic applications of receiver operating characteristic (ROC) curves. Radiology 110:89–95
Guzzetti F, Carrara A, Cardinali M, Reichenbach P (1999) Landslide hazard evaluation: a review of current techniques and their application in a multi-scale study, Central Italy. Geomorphology 31:181–216
Guzzetti F, Reichenbach P, Cardinali M, Galli M, Ardizzone F (2005) Probabilistic landslide hazard assessment at the basin scale. Geomorphology 72:272–299
Guzzetti F, Reichenbach P, Ardizzone F, Cardinali M, Galli M (2006) Estimating the quality of landslide susceptibility models. Geomorphology 81:166–184
Hanley JA, McNeil BJ (1982) The meaning and use of the area under a receiver operating characteristic (ROC) curve. Radiology 143:29–36
Hosmer DW, Lemeshow S (2000) Applied logistic regression, Wiley series in probability and statistics. Wiley, New York
Irigaray C, Fernández T, El Hamdouni R, Chacón J (2007) Evaluation and validation of landslide-susceptibility maps obtained by a GIS matrix method: examples from the Betic Cordillera (southern Spain). Nat Hazards 41:61–79
Jenness J (2006) Topographic position index (tpi_jen.avx) extension for ArcView 3.x, v. 1.3a. Jenness Enterprises. Available at: http://www.jennessent.com/arcview/tpi.htm.
Jiménez-Peralvárez J, Irigaray C, El Hamdouni R, Chacón J (2009) Building models for automatic landslide susceptibility analysis, mapping and validation in ArcGIS. NatHazards 50:571–590
Lasko TA, Bhagwat JG, Zou KH, Ohno-Machado L (2005) The use of receiver operating characteristic curves in biomedical informatics. J Biomed Inform 38:404–415
Lee S, Ryu JH, Won JS, Park HJ (2004) Determination and application of the weights for landslide susceptibility mapping using an artificial neural network. Eng Geol 71:289–302
Märker M, Pelacani S, Schröder B (2011) A functional entity approach to predict soil erosion processes in a small Plio-Pleistocene Mediterranean catchment in Northern Chianti, Italy. Geomorphology 125:530–540
Mathew J, Jha VK, Rawat GS (2009) Landslide susceptibility mapping and its validation in part of Garhwal Lesser Himalaya, India, using binary logistic regression and receiver operating characteristic curve method. Landslides 6:17–26
Mc Fadden D (1979) Quantitative methods for analyzing travel behavior of individuals: some recent developments. In: Hensher DA, Stopher PR (eds) Behavior travel modeling. Croom Helm, London, pp 279–318
Nagelkerke NJD (1991) A note on a general definition of the coefficient of determination. Biometrika 78:691–693
Nandi A, Shakoor A (2009) A GIS-based landslide susceptibility evaluation using bivariate and multivariate statistical analyses. Eng Geol 110:11–20
Nefeslioglu H, Gokceoglu C, Sonmez H (2008) An assessment on the use of logistic regression and artificial neural networks with different sampling strategies for the preparation of landslide susceptibility maps. Eng Geol 97:171–191
Ohlmacher GC, Davis JC (2003) Using multiple logistic regression and GIS technology to predict landslide hazard in northeast Kansas, USA. Eng Geol 69:331–343
Olaya V (2004) A gentle introduction to SAGA GIS. Göettingen, Germany
O'Callaghan JF, Mark DN (1984) The extraction of drainage network from digital elevation data. Comput Vision Graph 28:323–344
Pradhan B, Lee S (2010) Regional landslide susceptibility analysis using back-propagation neural network model at Cameron Highland, Malaysia. Landslides 7:13–30
Rakotomalala R (2005) Tanagra: un logiciel gratuit pour l'enseignement et la recherche. Actes De EGC:pp 697–702
Reineking B, Schröder B (2006) Constrain to perform: regularization of habitat models. Ecol Model 193:675–690
Rossi M, Guzzetti F, Reichenbach P, Mondini AC, Peruccacci S (2010) Optimal landslide susceptibility zonation based on multiple forecasts. Geomorphology 114:129–142
Rotigliano E, Agnesi V, Cappadonia C, Conoscenti C (2011) The role of the diagnostic areas in the assessment of landslide susceptibility models: a test in the Sicilian chain. Nat Hazards 58:981–999
Rotigliano E, Cappadonia C, Conoscenti C, Costanzo D, Agnesi V (2012) Slope units-based flow susceptibility model: using validation tests to select controlling factors. Nat Hazards 61:143–153
Süzen ML, Doyuran V (2004) A comparison of the GIS based landslide susceptibility assessment methods: multivariate versus bivariate. Environ Geol 45:665–679
Van Den Eckhaut M, Vanwalleghem T, Poesen J, Govers G, Verstraeten G, Vandekerkhove L (2006) Prediction of landslide susceptibility using rare events logistic regression: a case study in the Flemish Ardennes (Belgium). Geomorphology 76:392–410
Van Den Eeckhaut M, Reichenbach P, Guzzetti F, Rossi M, Poesen J (2009) Combined landslide inventory and susceptibility assessment based on different mapping units: an example from the Flemish Ardennes, Belgium. Nat Hazard Earth Sys 9:507–521
Vergari F, Della Seta M, Del Monte M, Fredi P, Lupia Palmieri E (2011) Landslide susceptibility assessment in the Upper Orcia Valley(Southern Tuscany, Italy) through conditional analysis: a contribution to the unbiased selection of causal factors. Nat Hazard Sys 11:1475–1497
Vorpahl P, Elsenbeer H, Märker M, Schröeder B (2012) How can statistical models help to determine driving factors of landslides? Ecol Model 239:27–39
Wilson JP, Gallant JC (2000) Terrain analysis: principles and applications. Wiley, Canada

D. Costanzo · C. Conoscenti · E. Rotigliano (✉)
Department of Earth and Sea Sciences,
University of Palermo, Italy,
Via Archirafi, 20-90123 Palermo, Italy
e-mail: edoardo.rotigliano@unipa.it

J. Chacón · C. Irigaray
Department of Civil Engineering, ETSICCP,
University of Granada, Spain,
Campus Fuentenuevac/Severo Ochoa s/n, 18071 Granada, Spain